Crystal structure of MltA from Escherichia coli reveals a unique lytic transglycosylase fold

van Straaten, K.E.; Dijkstra, B.W.; Vollmer, W.; Thunnissen, A.M.W.H.

Published in:
Journal of Molecular Biology

DOI:
10.1016/j.jmb.2005.07.067

Publication date:
2005

doi:10.1016/j.jmb.2005.07.067 J. Mol. Biol. (2005) 352, 1068–1080

JMB

Available online at www.sciencedirect.com

SCIENCE DIRECT®

ELSEVIER

Crystal Structure of MltA from *Escherichia coli* Reveals a Unique Lytic Transglycosylase Fold

Karin E. van Straaten[1], Bauke W. Dijkstra[1], Waldemar Vollmer[2] and Andy-Mark W. H. Thunnissen*

[1]*Laboratory of Biophysical Chemistry and Groningen Biomolecular Sciences and Biotechnology Institute University of Groningen Nijenborgh 4, 9747 AG Groningen, The Netherlands*

[2]*Department of Microbial Genetics, University of Tübingen, Auf der Morgenstelle 28, 72076 Tübingen, Germany*

**Corresponding author*

Lytic transglycosylases are bacterial enzymes involved in the maintenance and growth of the bacterial cell-wall peptidoglycan. They cleave the β-(1,4)-glycosidic bonds in peptidoglycan forming non-reducing 1,6-anhydro-muropeptides. The crystal structure of the lytic transglycosylase MltA from *Escherichia coli* without a membrane anchor was solved at 2.0 Å resolution. The enzyme has a fold completely different from those of the other known lytic transglycosylases. It contains two domains, the largest of which has a double-psi β-barrel fold, similar to that of endoglucanase V from *Humicola insolens*. The smaller domain also has a β-barrel fold topology, which is weakly related to that of the RNA-binding domain of ribosomal proteins L25 and TL5. A large groove separates the two domains, which can accommodate a glycan strand, as shown by molecular modelling. Several conserved residues, one of which is in a position equivalent to that of the catalytic acid of the *H. insolens* endoglucanase, flank this putative substrate-binding groove. Mutation of this residue, Asp308, abolished all activity of the enzyme, supporting the direct participation of this residue in catalysis.

Keywords: bacterial cell-wall peptidoglycan; lytic transglycosylase; double-psi β-barrel; glycoside hydrolase; X-ray crystallography

Introduction

Peptidoglycan (or murein) is a bacterial biopolymer composed of linear polysaccharide chains of alternating *N*-acetylglucosamine (GlcNAc) and *N*-acetylmuramic acid (MurNAc) residues cross-linked by short peptides attached to the D-lactyl groups of MurNAc residues. It forms a bag-shaped structure, the murein sacculus, which completely encloses the bacterial cell. The murein sacculus maintains the shape and size of the cell, providing mechanical support and protecting the bacterium from osmotic lysis.[1] The importance of peptidoglycan is highlighted by the fact that penicillin and related β-lactams, which interfere with its biosynthesis, are very effective and widely applied antibacterials, causing cell lysis and death.

β-Lactam antibiotics inhibit the so-called penicillin-binding proteins, which are responsible for the making and breaking of the peptide cross-linkages in peptidoglycan. These proteins are ideal targets for antibiotics, since peptidoglycan is essential and unique to bacteria. However, the rapid spread of resistance against these and other antibiotics is causing a serious health problem, creating an urgent need for alternative antibiotics and new antibiotic targets. Such new targets could be the β-lactam-insensitive lytic transglycosylases, which act on the glycosidic bonds in peptidoglycan, and which participate in peptidoglycan maintenance and processing as required, for example, during cell septation and division.[1–4] Specifically, these enzymes cleave the β-(1,4)-glycosidic bond between the MurNAc and GlcNAc residues in the peptidoglycan, forming non-reducing 1,6-anhydro-muropeptides. This is in contrast to the action of lysozyme, which cleaves the same bonds but produces muropeptides with free reducing ends. In *Escherichia coli*, at least six different lytic transglycosylases have been identified and functionally characterized: one soluble (Slt70) and five that are outer membrane-bound (MltA-MltD, EmtA).[4–6] Genomic analyses indicate that lytic transglycosylase sequences are widespread among

Abbreviations used: GlcNAc, *N*-acetylglucosamine; MurNAc, *N*-acetylmuramic acid; MltA, membrane-associated lytic transglycosylase A; sMltA, soluble form of MltA; Slt70, 70 kDa soluble lytic transglycosylase; EGV, endoglucanase V; GH, glycoside hydrolase.

E-mail address of the corresponding author: a.m.w.h.thunnissen@rug.nl

bacteria and are found in certain bacteriophages,[7] although the functional information on these hypothetical lytic transglycosylases is rather limited. The important role of the lytic transglycosylases in murein metabolism is underlined by the observation that bulgecin A, which is a specific inhibitor of the *E. coli* lytic transglycosylases Slt70, MltC and MltD,[8,9] enhances the efficacy of β-lactam antibiotics.[10,11]

The lytic transglycosylases from *E. coli* share only little sequence homology with each other. On the basis of differences in signature sequence motifs around their catalytic regions they have been classified into four families.[7] Lytic transglycosylase family 1 forms a superfamily containing four subfamilies of proteins with amino acid sequence similarity to Slt70, MltC, MltD, and EmtA. The other two *E. coli* lytic transglycosylases, MltA and MltB, constitute families 2 and 3, respectively, which are not related to each other or to family 1. Finally, lytic transglycosylase family 4 comprises mostly enzymes encoded by λ bacteriophages. Structural research on the *E. coli* lytic transglycosylases has so far resulted in the X-ray structures of the family 1 lytic transglycosylases Slt70[12,13] and EmtA (F. Gliubich & A.-M.W.H.T., unpublished results), and of a soluble fragment of MltB from the lytic transglycosylase family 3.[14] Despite differences in overall structure, all these structurally characterized enzymes share a catalytic domain that resembles the fold of goose-type lysozyme,[14,15] classifying them as members of glycoside hydrolase family 23.[16] This lysozyme-like catalytic domain is recognizable also in the crystal structure of the lytic transglycosylase from bacteriophage λ,[17,18] although it is more divergent from goose-type lysozyme than the catalytic domains of the lytic transglycosylases Slt70, Slt35 and EmtA. Binding studies with murein-derived compounds gave insight into the interactions of the enzymes with oligosaccharides, and defined the location and number of the saccharide-binding sites.[13,18–20] These investigations, combined with site-directed mutagenesis experiments, indicated the important role of a glutamate residue in the catalytic mechanism of the family 1, family 3 and family 4 lytic transglycosylases, and suggested that this residue functions as the catalytic acid/base similar to Glu73 in goose-type lysozyme. So far, no structure of a member from lytic transglycosylase family 2 has been solved.

To increase our knowledge of the molecular details of the cleavage mechanism and typical 1,6-anhydro-muropeptide production by the *E. coli* lytic transglycosylases, we initiated a structural study of the family 2 lytic transglycosylase MltA from *E. coli* by X-ray crystallography. Mature MltA has a molecular mass of 38 kDa, and is composed of 345 amino acid residues.[21] It lacks the family 1 lytic transglycosylase sequence motifs that characterize the catalytic lysozyme-like domain. Furthermore, it differs from Slt70 and MltB, in that it is capable of degrading both insoluble murein sacculi and isolated poly(MurNAc-GlcNAc) glycan strands.[21] Sequence comparison of *E. coli* MltA with MltA-like enzymes from other Gram-negative bacteria shows that there is no conserved glutamate present, but that there are three invariant aspartic acid residues.[7] Since the optimal activity of MltA is between pH 4.0 and pH 4.5, this suggests that one of these three conserved aspartic acid residues might serve as the catalytic acid/base. Here, we report the structure of the *E. coli* lytic transglycosylase MltA, as determined by X-ray crystallography at 2.0 Å resolution. This is the first reported structure of a family 2 lytic transglycosylase. It shows a novel lytic transglycosylase fold, which is markedly different from that of the other lytic transglycosylases, but which resembles the fold of endoglucanase V from *Humicola insolens*, a glycoside hydrolase family 45 enzyme.[16]

Results and Discussion

Structure solution

Mature wild-type MltA is anchored to the outer membrane of *E. coli via* a lipoyl moiety attached to its N-terminal cysteine residue. To facilitate its crystallization, a fully functional, recombinant, soluble form of MltA (sMltA) was created by deleting the N-terminal signal sequence and replacing the N-terminal cysteine residue with a methionine residue. sMltA was purified and crystallized, and its structure was determined at 2.0 Å resolution to a final *R*-factor of 20.7% and an R_{free} of 23.7%, with good overall geometry (Table 1). The electron density is well defined for the whole range of the polypeptide chain, except for the first two residues at the N terminus and the last eight C-terminal residues. These residues are not visible in the $2F_o-F_c$ electron density map and were therefore not included in the final model. Residue 131 appeared to be serine rather than the proline residue present in the *E. coli* genome sequence. DNA sequencing confirmed the presence of a serine residue at this position, which most likely is an artefact of the cloning procedure. Residue 131 is located at the surface of the molecule, far from the putative active site and the substitution is therefore not believed to have structural or functional consequences.

Overall structure

sMltA is a kidney bean-shaped monomeric protein with dimensions of approximately 70 Å × 35 Å × 30 Å. It contains two domains (A and B) separated by a large groove approximately 35 Å long and 14 Å wide (Figure 1). Domain A is composed of two discontinuous amino acid sequence segments (residues 3–104 and 244–337) and consists of an N-terminal part (residues 3–90) and a β-barrel core. The N-terminal part contains two antiparallel β-strands (β1 and β2) connected by

Table 1. Data collection and refinement studies

	Selenomethionine-labelled			
Crystal	Inflection	Peak	Remote	Native
A. *Data collection*				
Wavelength (Å)	0.9494	0.9792	0.9393	0.9393
Space group	$P3_121$			$P3_121$
Unit cell axes				
a (Å)	103.6			103.9
b (Å)	103.6			103.9
c (Å)	110.3			109.8
Resolution range[a] (Å)	30–2.6 (2.1–2.6)	30–2.6 (2.7–2.6)	30–2.6 (2.7–2.6)	30–2.0 (2.1–2.0)
Completeness[a] (%)	98 (85)	99 (88)	94 (59)	100 (100)
Redundancy[a]	5.3 (3.9)	5.5 (3.9)	4.9 (4.8)	5.6 (5.6)
Mean $I/\sigma I$[a]	9.5 (1.7)	10.0 (2.0)	5.9 (0.9)	10 (1.6)
R_{merge}[a] (%)	8.1 (45)	8.6 (31)	11.9 (69)	4.8 (49)
B. *Refinement*				
Resolution range (Å)				30–2.0
No. unique reflections				44,258
No. amino acid residues				335
No. protein atoms				2637
No. solvent atoms				292
Root-mean-square deviations				
Bond lengths (Å)				0.004
Bond angles (deg.)				1.12
Ramachandran plot				
Most-favoured (%)				91
Additionally allowed (%)				9
R_{work}[b] (%)				20.7
R_{free}[c] (%)				23.7

[a] Data between parentheses are for the highest resolution shell.
[b] $R_{work} = \sum_{hkl} ||F_{obs}| - |F_{calc}|| / \sum_{hkl} |F_{obs}|$, where the crystallographic *R*-factor was calculated with 95% of the data used in the refinement.
[c] R_{free} is the crystallographic *R*-factor based on 5% of the data withheld from the refinement for cross-validation.

three helices (α1–α3). Strand β2 is also hydrogen bonded to β14 of the β-barrel of domain A. This β-barrel is the main feature of domain A and consists of a mixed parallel/antiparallel six-stranded closed β-barrel made of β-strands β3 and β10–β14, with one small α-helix (α9) (Figure 1(a) and (b)). The β-barrel has a double-psi β-barrel fold, as classified by SCOP.[22] This fold consists of two interlocked "psi-structure" motifs related by a pseudo-2-fold axis. In MltA, these psi-structure motifs are β10, β11, β12 and β13, β14, β3 (Figure 1(b)). They are characterized by two antiparallel β-strands connected by a loop (a psi-loop) with a third β-strand inserted between them, thus resembling the Greek letter ψ. There are a number of structural features that typify this fold.[23] Side-chains on β-strands that point to the interior of the barrel are predominantly hydrophobic (i.e. Val258, Leu271, Ala273, Val275, Met293 and Ala295 in the first half of the barrel, and Phe307, Val330 and Val332, Val96 and Phe98 in the second half (Figure 2)). Conserved positive phi angles are required in the turns that precede the equivalent β-strands 11 and 14 (i.e. Gly268 (phi = 90°, psi = −10°) and Gly322 (phi = 70°, psi = −180°). Residues at the C-terminal ends of β10 and β13 play a key role in positioning β10 and β13 under their respective psi-loops, and in linking these strands to the immediate subsequent regions in the polypeptide. For instance, the side-chain of Asp261 at the C-terminal end of β10 is hydrogen bonded to the main-chain NH of Gly304 in the second psi-loop and to the O^{γ} and main-chain NH of Ser263 in the β10-β11 loop. Similarly, at the C-terminal end of β13, the Tyr310-OH group is able to make a hydrogen bond with the side-chain of Thr103 in the first psi-loop. In addition, the main-chain oxygen atom of Gly312 is within hydrogen bonding distance from the main-chain NH of Thr103 in the first psi-loop, while the main-chain carbonyl oxygen atom and the side-chain O^{ε} of Gln311 form hydrogen bonds with the side-chain Arg320 of α9.

Domain B (residues 105–243) is inserted between strands β3 and β10 of sMltA. It contains a small mixed parallel/antiparallel six-stranded β-barrel (β4-β9), but with a different topology compared to the β-barrel topology of domain A (Figure 1(c)). A DALI[24] search of the protein data bank for similar folds revealed a weak structural similarity with the β-barrel present in the RNA-binding domain of the ribosomal proteins L25 from *E. coli* and TL5 from *Thermus thermophilus* (Figure 3(b)).[25,26] In these proteins, the β-barrel is composed of two approximately perpendicular β-sheets, which each contain one antiparallel and two parallel β-strands. In one of the sheets, the outer strands are bent and shared with the other sheet, thus creating a closed barrel. This topology is essentially conserved in domain B of sMltA, including the presence of an α-helix (α5),

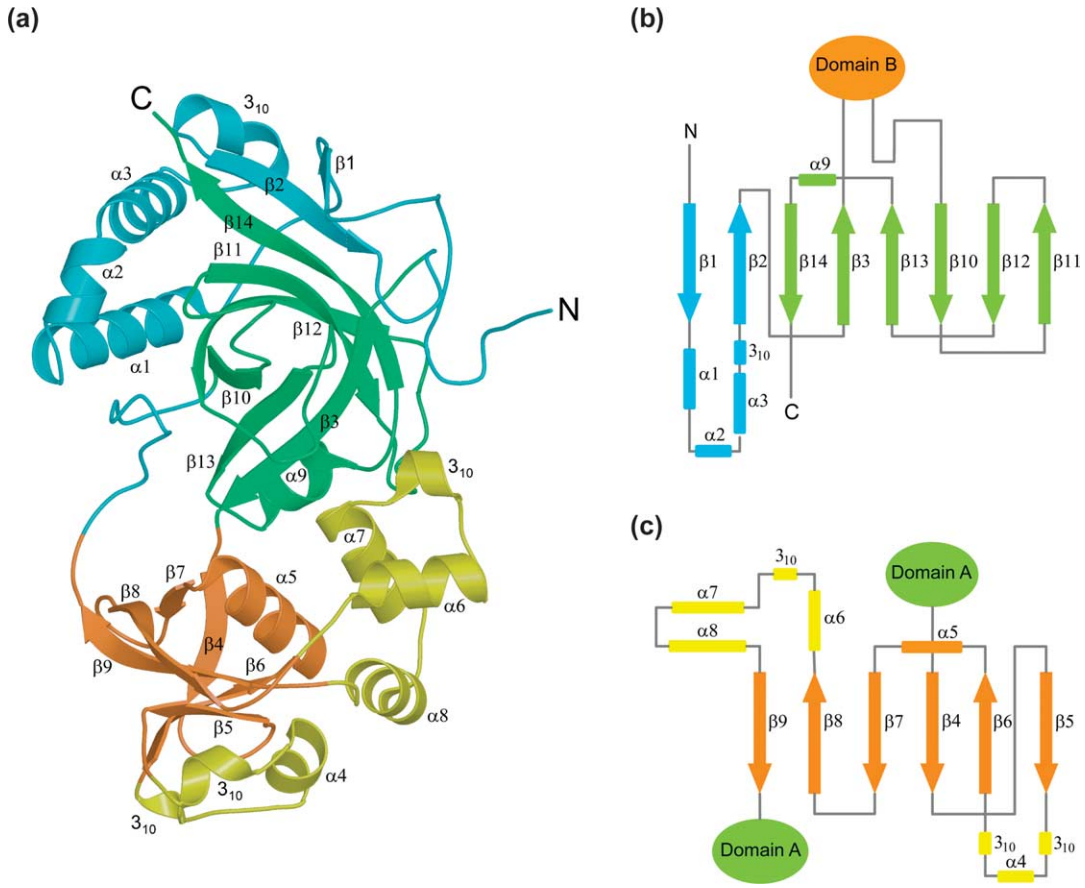

Figure 1. Crystal structure and topology of sMltA. (a) The overall structure of sMltA shown as a ribbon diagram. Domain A is shown in blue and green, domain B is shown in yellow and orange, with the double-psi and TL5 related β-barrel folds highlighted in green and orange, respectively. Secondary structure elements are indicated. (b) Idealized topology diagram of domain A of sMltA. (c) Similar topology diagram of domain B of sMltA (colors as in (a)).

inserted between the third and fourth strand, which caps one end of the β-barrel. Unlike the barrels in L25 and TL5, however, the barrel in sMltA is highly distorted, due to the strands being shorter and having shifted compared to their equivalents in L25 or TL5. In particular, strands β5 and β9 in sMltA (the equivalents of strands β2. and β6, respectively, in TL5) are widely separated and have just one inter-strand hydrogen bond interaction, which results in the barrel being partially open at one side. Four additional α-helices are found in domain B of sMltA, which have no equivalent in the L25 or TL5 RNA-binding domains. Three of these helices (α6, α7 and α8) form, together with a short 3_{10}-helix, the connection between strands β8 and β9. Together with helix α5, they define a small helical sub-domain, which participates in a number of non-covalent interactions with domain A, thus stabilizing the relative orientations of the two sMltA domains. The absence of any significant sequence similarity, the relative displacements of equivalent β-strands and the highly divergent inter-strand connecting regions (with the exception of one helix) demonstrate the limited nature of the overall structural homology between domain B of sMltA and the ribosomal proteins, making the presence of any functional relationships highly unlikely.

A novel lytic transglycosylase fold belonging to the barwin-like endoglucanase family

Comparison of the sMltA structure with the 3D structures of the other lytic transglycosylases showed the absence of any structural similarity, which was corroborated through a DALI search. sMltA does not possess the characteristic α-helical lysozyme-like fold of the other four lytic transglycosylases. Instead, sMltA is mainly a β-protein. From this, we conclude that the structure of MltA represents a new lytic transglycosylase fold, and that MltA has evolved from a different ancestor than the other lytic transglycosylases. Because of this lack of structural similarity, the other lytic transglycosylases cannot help us in identifying the active site of MltA and the residues participating in substrate binding and catalysis. However, a CATH[27] search with domain A of sMltA revealed a structural relationship to the barwin-like endoglucanase superfamily, with greatest similarity to the catalytic domain of endoglucanase V from *Humicola insolens*. Endoglucanase V (EGV) is a cellulase that cleaves the β-(1,4)-glycosidic bonds of cellulose with inversion of configuration.[28]

To quantify the similarity between the equivalent domains of MltA and EGV, the two domains were

superposed (Figure 3(a)). A total of 59 C^{α} atoms, representing 30% of the C^{α} atoms of domain A, overlap with the EGV barrel, with a root-mean-square difference of 1.5 Å. A structure-based sequence alignment of the two domains (Figure 2) shows that 12 residues are identical. Two of these conserved residues, Gly304 and Phe307 (MltA numbering), stabilize the double-psi β-barrel fold, while the other ten identical residues (Thr99, Tyr101, Lys245, Ala259, Gly299, Gly300, His306, Asp308, Gly314 and Asn325) all point into the groove that separates the two sMltA domains. In EGV, seven of these ten identical residues are involved in substrate binding, one being an aspartic acid residue (Asp121) that functions as the catalytic acid in the mechanism of cellulose hydrolysis.[29,30] Its equivalent residue in sMltA is Asp308, which is located centrally in the groove, and which is absolutely conserved in all known MltA sequences. The structural equivalences and conservation of functionally important residues point strongly to a role of the groove in sMltA in binding the glycan strands of the murein substrate, with Asp308 functioning as proton donor in the mechanism of cleavage of the β-(1,4)-glycosidic bonds.

Peptidoglycan binding groove and active site

The similar arrangement of the β-strands in the double-psi β-barrel and the significant, although low, amino acid sequence conservation argue for a possible common evolutionary origin of MltA and EGV. If this is the case, then the active sites of the two proteins are likely to be found in similar locations, and substrates would be expected to bind in a similar way in MltA and EGV. In addition, one would anticipate the occurrence of specific deletions, insertions and side-chain alterations to be related to differences in substrate specificity and reaction mechanism. In all known protein structures with a double-psi β-barrel the active site clusters around the ψ-loops.[23] In EGV (and by implication also in sMltA) the ψ-loops border the substrate-binding groove. Crystallographic binding studies with cellulose fragments showed that the substrate-binding groove in EGV spans from subsite −4 to subsite +3, with glycosidic bond cleavage taking place between the +1 and −1 subsites (Figure 3(a)).[30] To gain insight into the mechanism of substrate binding and cleavage by MltA, a short glycan chain was modelled in the sMltA groove, using the structure of EGV with two bound cellotriose molecules as a template. As shown in Figure 4, the sMltA groove is long enough to accommodate a six residue-long glycan chain, with the sugar rings occupying positions equivalent to those of subsites −3 to +3 in EGV. The substrate-binding groove in sMltA, however, is significantly wider than that in EGV, primarily due to a reduced number of protruding loop regions in sMltA (Figures 3(a) and 4(b)). In EGV, these loop regions (i.e. residues 10–12, 36–54, 128–132 and 146–149) participate in substrate binding, and their absence from sMltA causes the sugars occupying subsites −3, −2 and −1 to be largely solvent-exposed, while subsite −4 is completely absent. The sugars occupying subsites +1, +2 and +3 in sMltA, on the other hand, are less accessible to solvent, since in that region of the substrate-binding groove the helical subdomain of domain B participates in formation of the sugar subsites. In fact, at subsite +2 the binding groove in sMltA becomes quite narrow due to inter-domain contacts, causing the passage to subsite +3 to be blocked for a polysaccharide chain entering from the direction of the neighbouring subsites, possibly explaining the exolytic activity reported for this enzyme.[21] The absence from sMltA of equivalents to some of the substrate-binding loops of EGV may be correlated to the difference in substrate specificity between these two enzymes. At subsites −2 and +1 in sMltA, they create, together with a few occurrences of shorter side-chains at equivalent positions, the extra space needed for accommodating the *N*-acetyl groups of the sugar moieties (Figure 4(b)). The position of the sugar rings in subsites −2 and +1, with their C2 and C3 substituents buried in the groove, is incompatible with the presence of a D-lactyl group attached to the O3 atom, suggesting that in MltA at these subsites only GlcNAc, but not MurNAc residues, can bind. Because in peptidoglycan GlcNAc and MurNAc residues alternate, this implies that MurNAc residues bind at subsites −3, −1 and +2, with their lactyl moiety pointing outwards from the groove.

The conserved Asp308 is situated near the −1 and +1 subsites, at hydrogen bonding distance to the O4 atom of the glycosidic bond connecting MurNAc −1 and GlcNAc +1, in agreement with a role as proton donor in the cleavage step of the lytic transglycosylase reaction. Interestingly, although there are two additional, strictly conserved aspartate residues in sMltA (Asp261 and Asp297, Figure 4(a)), none of them corresponds to the catalytic base of EGV (Asp10), nor is there another basic residue in sMltA equivalent to Asp10 of EGV. This may suggest that, like the single catalytic glutamic acid residue in the catalytic mechanism of the family 1, family 3, and family 4 lytic transglycosylases, Asp308 also functions as a single catalytic acid/base in MltA. To further test this hypothesis, the three strictly conserved aspartate residues in sMltA (Asp261, Asp297, and Asp308) were mutated into alanine by site-directed mutagenesis, and the activities of the mutant proteins were compared to that of the original protein (Table 2). Replacement of Asp308 by Ala resulted in a complete loss of activity within the accuracy of the experiment (residual activity as low as 1%), confirming its crucial role in catalysis. The activity of the Asp297Ala mutant was also strongly reduced, but significant residual activity remained, showing that Asp297 is not absolutely essential for catalytic activity. Most likely, this residue participates in substrate binding, considering its location near subsite −2 (Figure 4).

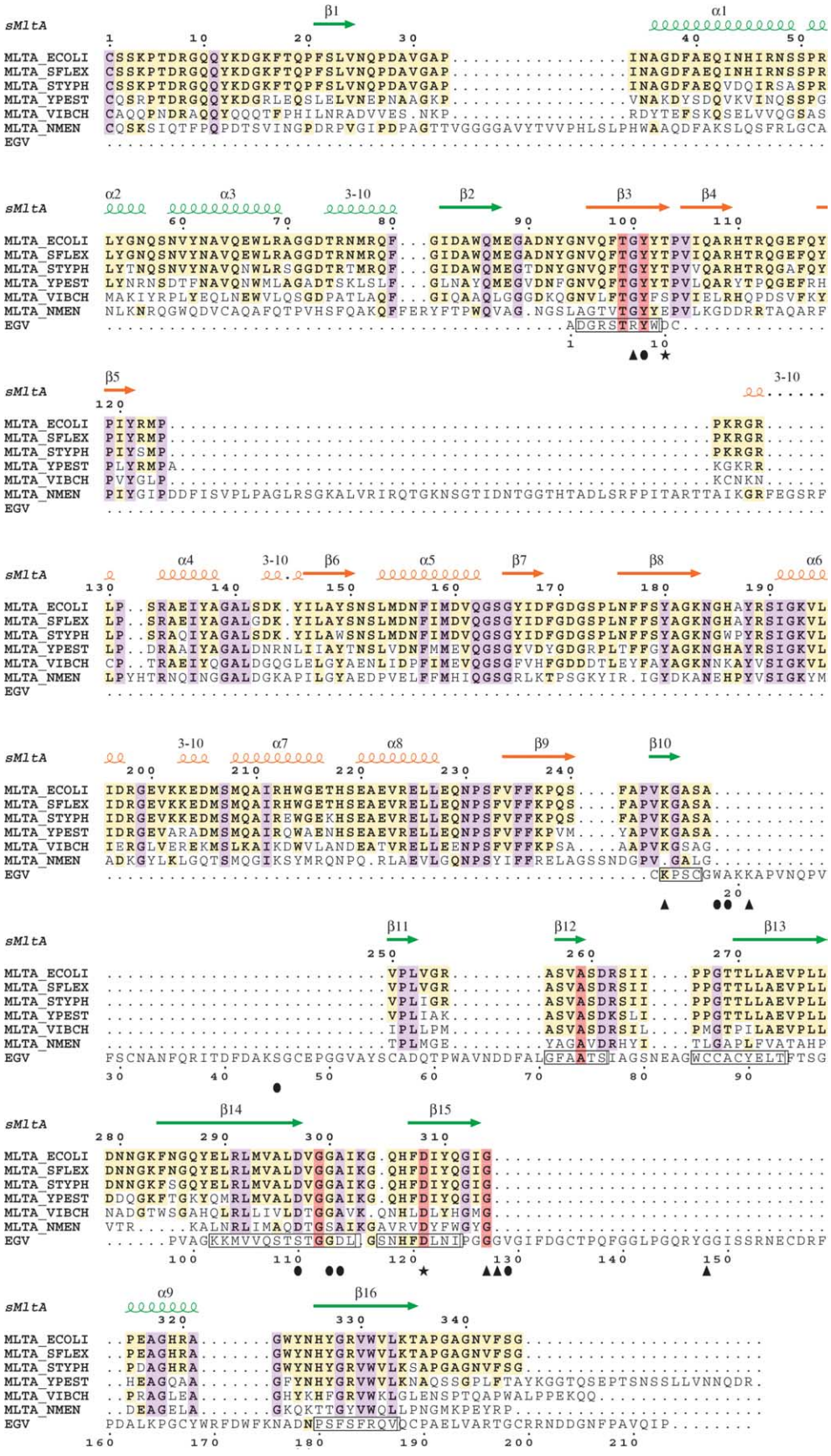

Figure 2. Sequence and structural homology of MltA. The sequence of MltA from *E. coli* (labelled MLTA_ECOLI) was aligned with five other MltA sequences from different organisms, as well as with the sequence of endoglucanase V from *H. insolens*. The additional MltA sequences are from *Shigella flexneri* (MLTA_SFLEX), *Salmonella typhimurium*

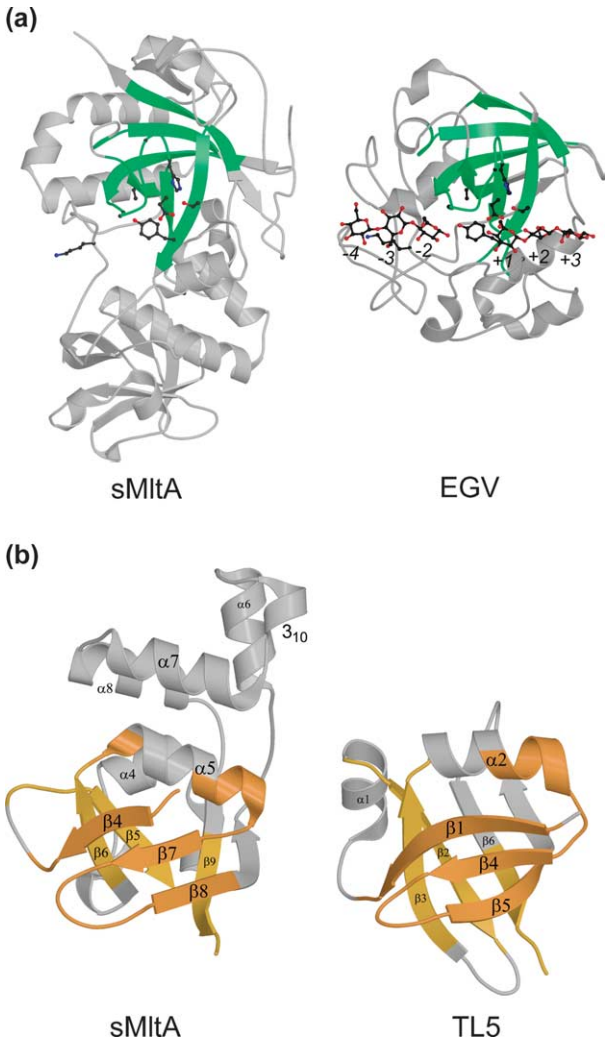

Figure 3. Comparison of sMltA to related structures. (a) Ribbon representations of the structure of sMltA and the structure of EGV in complex with two cellotriose molecules (Protein Data Bank entry 4ENG) shown in identical orientations. The common cores are coloured green. Identical residues (based on Figure 2) are shown in ball-and-stick representations. (b) Ribbon representations of the structures of domain B of sMltA and of the RNA-binding domain of TL5 (Protein Data Bank entry 1FEU) shown in identical orientations. The common cores are coloured orange. Superpositions were calculated using LSQMAN (http://xray.bmc.uu.se).

The activity of the Asp261Ala mutant is least affected, indicating that this residue is not very important for the activity of MltA. It is located near the C-terminal end of β12 and points away from the groove and it therefore would not interfere with substrate binding.

Functional implications

Previous studies of the lytic transglycosylases Slt70 and MltB showed that the reaction catalyzed by these enzymes most likely takes place *via* a general acid/base mechanism that requires participation of a single catalytic residue, i.e. Glu478 in Slt70 and Glu162 in MltB.[13–15,19,20] In the first step of the reaction, the catalytic glutamic acid residue donates a proton to the oxygen atom of the scissile glycosidic bond, resulting in bond breakage and formation of an oxocarbenium ion intermediate. In the second step, the same catalytic residue serves as a base activating the oxygen atom of the C6 hydroxyl group of the −1 MurNAc residue for an intramolecular nucleophilic attack on the anomeric C1 carbon atom, resulting in formation of a β-1,6-anhydro bond.[31] This mechanism classifies the lytic transglycosylases as retaining β-glycosidases. However, their reaction mechanism is uniquely different from the general reaction mechanism of retaining β-glycosidases, which in addition to an acid/base catalyst requires either participation of a second catalytic carboxylate group functioning as a nucleophile in the first step of the reaction,[16,32] or anchimeric assistance by a substrate *N*-acetyl group.[33,34] In retaining β-glycosidases, this second group attacks the −1 sugar from the α-face of the C1 carbon centre, resulting in formation of a covalent glycosyl-enzyme or covalent oxazoline intermediate. In the second step, this covalent intermediate is then attacked by a water molecule from the β-face of the C1 carbon, thus releasing the free reducing sugar. Formation of a covalent intermediate is an essential part of the general mechanism of retaining β-glycosidases, as the lifetime of an oxocarbenium ion intermediate is too short to allow the replacement at the active site of the leaving group with a water molecule. The lytic transglycosylase reaction, on the other hand, does not require such a replacement, so there is no need for a substantial increase in lifetime of the intermediate, and this could explain the absence of a second catalytic carboxylate group in the active site. Alternatively, the C2 acetamido group of the −1 MurNAc residue

(MLTA_STYPH), *Yersinia pestis* (MLTA_YPEST), *Vibrio cholerae* (MLTA_VIBCH) and *Neisseria meningitidis* (MLTA_NMEN). The multiple sequence alignment was guided by a structural alignment of sMltA and EGV (Protein Data Bank entry 2ENG). The common core between these two structures is indicated with black boxes around residues of the EGV sequence. Residues that are identical in all seven sequences (including EGV) are shaded with red, while residues that are identical in all six MltA sequences (but not in the EGV sequence) are shaded with violet. Additional residues that are identical with residues in *E. coli* MltA are shaded with yellow. Residues in EGV that have a role in substrate binding and/or catalysis are indicated with different symbols: (▲) residues with a direct substrate-binding interaction, (●) residues with a water-mediated substrate-binding interaction, (*) catalytic residues. The secondary structure elements refer to the structure of sMltA. The Figure was prepared using ESPript.[53]

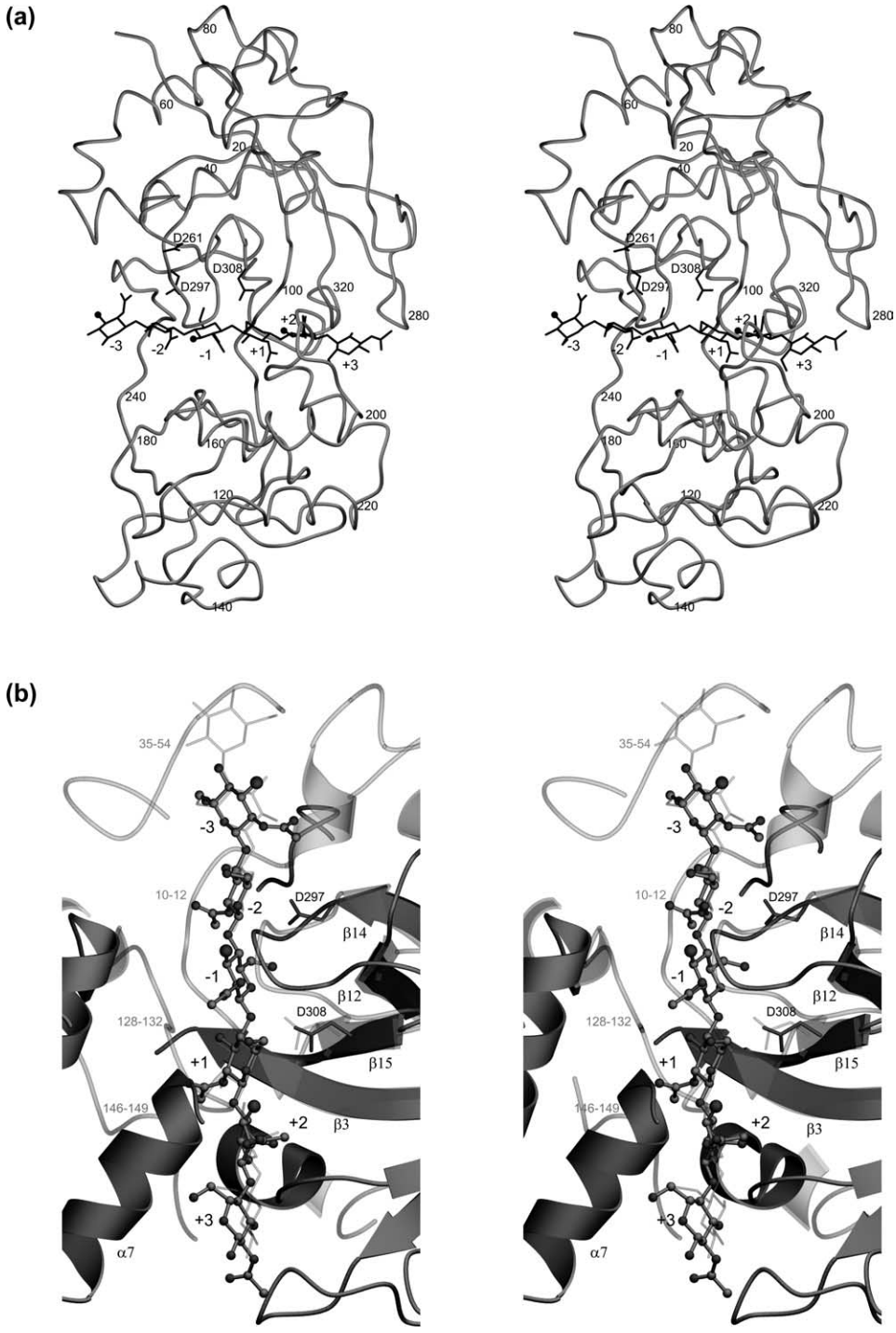

Figure 4. Structural details of the glycan-bound sMltA model. (a) Stereo representation of the C^{α} backbone of sMltA with a $(MurNAc\text{-}GlcNac)_3$ oligosaccharide modelled in the substrate-binding groove. The different sugar-binding subsites are indicated. For reasons of clarity, the O3-linked lactyl groups of the MurNAc residues were omitted from this Figure, and instead are indicated by spheres. In addition, the side-chains of the three strictly conserved aspartate residues in MltA are shown (Asp261, Asp297 and Asp308). (b) Stereo view of the superposition of the $(MurNAc\text{-}GlcNac)_3$-bound sMltA model and the $(GlcNAc)_3$-bound EGV structure, focusing on the equivalent substrate-binding groove regions. The glycan molecule is shown in ball-and-stick representation with the positions of the O3-linked lactyl groups of the MurNAc residues indicated by large spheres. The two cellotriose molecules bound to EGV are drawn with light grey lines. The backbone of sMltA is shown in dark grey, while the backbone of EGV is shown with a semi-transparent, light grey surface. Secondary structure labels refer to the sMLtA structure. Residue numbers in light grey indicate the substrate-binding loops in EGV that have no equivalent in sMltA. Also indicated in the sMltA structure are the side-chains of the catalytic Asp308 (and the equivalent residue in EGV), as well as of Asp297, which is in hydrogen bond distance from the *N*-acetyl group of the GlcNAc residue occupying subsite -2.

Table 2. Relative activity (%) of three sMltA mutants

Substrate	D261A	D297A	D308A
Murein sacculi	91(±6)	24(±2)	< 1
Glycan strands	90(±4)	32(±18)	< 1

The relative activity is defined as the percentage of activity remaining relative to the activity of unmodified sMltA with the same substrate. Values within parentheses are the estimated errors, based on multiple measurements.

or a carboxylate group in a neighbouring peptide moiety of the substrate may provide anchimeric assistance during catalysis, as suggested previously on the basis of the crystallographic analysis of different lytic transglycosylase–sugar complexes.[19,20] Apart from stabilizing an oxocarbenium ion intermediate, such groups may in addition act to shield the α-face of the oxocarbenium ion from solvent during the lytic transglycosylase reaction.

Our current analysis of the crystal structure of sMltA and the activities of the sMltA mutants indicate that this enzyme most likely utilizes a catalytic mechanism similar to that of the other lytic transglycosylases, even though their overall structures are completely unrelated (Figure 5). Indeed, the sMltA-glycan model shows that at subsite −1, Asp308 is in an position equivalent to that of the catalytic glutamic acid residues of Slt70 and MltB, and able to interact with the oxygen atom of the glycosidic bond that straddles the −1 and +1 subsites, and with the C6 hydroxyl group of the −1 MurNAc residue (Figure 4(b)). A surprising feature of the sMltA structure, though, is the open geometry of the peptidoglycan-binding groove, especially at subsites −3, −2 and −1. Our modelling study indicates that the sugar residues occupying these subsites remain largely accessible to solvent and may make significantly fewer interactions with protein atoms compared to those in the crystal structures of Slt70–sugar and MltB-sugar complexes. Most significantly, at subsite −1 the C1 carbon atom of the MurNAc residue is not shielded from the solvent by protein atoms, which seems incompatible with the lytic transglycosylation reaction performed by MltA. The geometry at the active site in the MltA-glycan model does not provide evidence for possible assistance in catalysis by the C2 acetamido group of the substrate. A catalytic involvement of the substrate's peptide moieties is also highly unlikely, as the activity of MltA, unlike that of Slt70 and MltB, does not depend on the presence of the peptide moieties in the substrate, as evident from previous functional studies,[21] as well as from the catalytic behaviour of sMltA and the three mutants in the current study. Decreasing the accessibility of the bound polysaccharide substrate and increasing the number of protein–sugar interactions may be accomplished by a conformational change that narrows the groove between domain A and domain B. The necessity of such a conformational change is further indicated by analysis of the distribution of conserved residues in domain B of the sMltA structure. As is evident from Figure 2, this domain shows a large number of residues that are strictly conserved among the different MltAs. A large fraction of these conserved residues are found near the peptidoglycan binding groove, suggesting that they have an important function in substrate binding (Figure 6). However, in the sMltA-glycan model they are too far from the expected position of the glycan chain to be able to make any interaction with the substrate. Therefore, we anticipate a reorientation of the two domains, which narrows the peptidoglycan binding groove, thus bringing these residues closer to

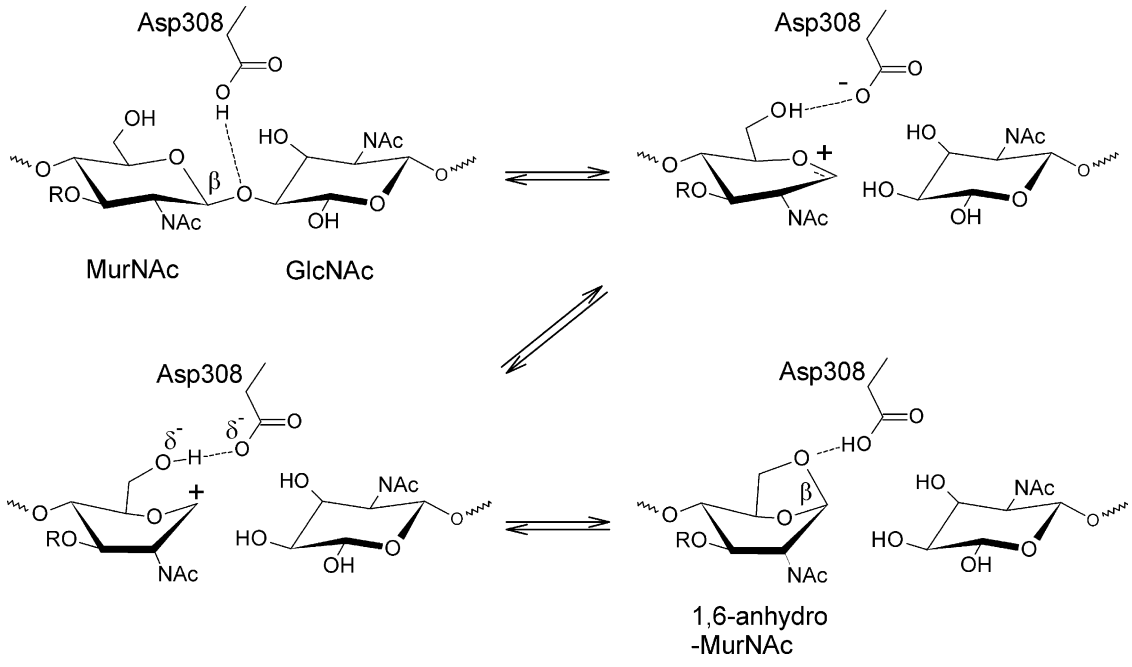

Figure 5. A representation of the proposed reaction mechanism of MltA.

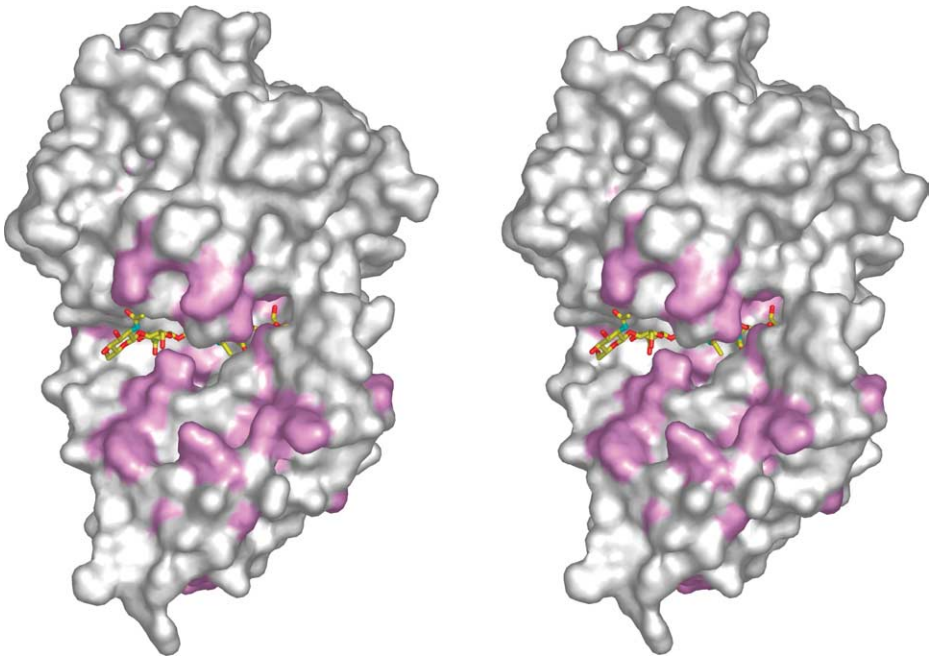

Figure 6. Surface representation of sMltA with the modelled glycan substrate. The modelled $(MurNAc\text{-}GlcNac)_3$ glycan substrate is shown in stick representation, with the lactyl groups on the MurNAc residues omitted for ease of illustration. Residues that are strictly conserved among the different MltA sequences are coloured violet. The Figure was drawn using PyMOL (http://www.pymol.org).

the sugar backbone of the substrate and prohibiting access of water near the C1 carbon atom of the sugar residue bound at subsite −1.

The structural and functional similarities between sMltA and EGV indicate that members of lytic transglycosylase family 2 belong to glycoside hydrolase (GH) family 45.[16] Surprisingly, though, all previously characterized members of GH family 45 are inverting endoglucanases. Furthermore, members of GH family 45 are structurally related to proteins like barwin[35] and plant expansins,[36] for which sugar-converting activities have not been detected. Interestingly, while the overall sequence identities are rather low, all these proteins have a conserved aspartate residue at the position of the catalytic acid/base of sMltA. This may signify an important structural role of this residue in stabilizing the double-psi β-barrel fold, or, alternatively, perhaps point to undiscovered catalytic functions for barwin and the plant expansins. The diversities in function further illustrate the versatility of the double-psi β-barrel fold and its potential as a scaffold onto which new functionalities may be grafted.

Summary and perspectives

The crystal structure of sMltA is the first structure of a member of lytic transglycosylase family 2, and reveals a fold completely different from those of the other known lytic transglycosylases. While the latter proteins share a catalytic core with a lysozyme-like fold, the catalytic domain of MltA contains a double-psi β-barrel, and has a fold similar to that found for members of the superfamily of barwin-like endoglucanases. Comparison to the catalytic core domain of endoglucanase V from *H. insolens*, combined with modelling and site-directed mutagenesis studies, allowed us to identify structural regions in sMltA that are involved in substrate binding and catalysis. In particular, our results point to an essential role for Asp308 as the single acid/base catalyst in the lytic transglycosylase reaction mechanism. This suggests that, despite the absence of structural homology, the reaction mechanism of MltA is similar to that of the other lytic transglycosylases. To obtain a full, detailed description of the MltA-peptidoglycan interactions and cleavage mechanism, and to evaluate a possible involvement in substrate binding of domain B of MltA, we have initiated crystallographic binding studies with various peptidoglycan-based and chitin-based fragments. Combined with the present structure of sMltA and the structural information available for the other lytic transglycosylases, these studies should enable a deeper understanding of the function of lytic transglycosylases and their role in bacterial cell-wall metabolism.

Materials and Methods

Purification and crystallization

The purification and crystallization of sMltA have been described.[37] A selenomethionine-substituted MltA variant (SeMet-sMltA) was prepared using *E. coli* cells grown in 2×M9 minimal medium, which was supplemented, 15 min before induction, with 46 mg/l of L-selenomethionine and a mixture of amino acids known to inhibit methionine biosynthesis.[38,39] Purification of

SeMet-sMltA was carried out as described for sMltA with 5 mM DTT included in all buffers to prevent oxidation of selenomethionine.[37] A yield of about 8 mg of pure protein was obtained from a 2 l culture. Single hexagonal rod-like crystals grew at 280 K, in about one to two weeks from 100 mM sodium acetate buffer (pH 4.2) containing 5–8% PEG 8000, 250–350 mM NaCl and 5 mM DTT, which are the same conditions as those used for the crystallization of the native protein.[37] Based on the analysis of the multiple anomalous dispersion (MAD) phasing data (see below), the space group to which the crystals belong was assigned as $P3_121$, with one molecule in the asymmetric unit and an estimated solvent content of about 72% (v/v).

Data collection and phasing

Diffraction data were collected at 100 K with 19% (v/v) ethylene glycol as a cryoprotectant in sodium acetate buffer (pH 4.2) containing 11% (w/v) PEG 8000, 350 mM NaCl, 100 mM and 5 mM DTT. A native data set to 2.0 Å resolution was measured on beam-line ID14-EH1 at the ESRF (Grenoble) using an unsubstituted sMltA crystal. For phasing, three-wavelength Se-MAD data to 2.6 Å resolution were collected from a single SeMet-sMltA crystal on beam line ID14-EH4 at the ESRF (Grenoble). All diffraction data were processed using the programs DENZO and SCALEPACK.[40] From the anomalous differences in the peak wavelength data, eight selenium sites were found by the SnB program,[41] in agreement with the presence of a single protein molecule in the asymmetric unit. Refinement of the selenium sites against the three-wavelength MAD data, and calculation of phases were carried out with the program SOLVE.[42] The MAD phases were improved by solvent flattening using the program RESOLVE,[42] assuming a solvent content of 70% (v/v).

Refinement

The electron density map calculated with the experimental phases was of sufficient quality to build a starting model of sMltA using the program Xfit from the XtalView[43] software package. Subsequently, this starting model, containing residues 8–337, was refined against the unsubstituted sMltA diffraction data. After an initial rigid-body refinement using Refmac5[44] (30–3.0 Å resolution) the model (R_{work} of 39.8%, R_{free} of 40.7%) was further refined using CNS.[45] Several rounds of simulated annealing, energy minimization and *B*-factor refinement, alternated with manual model rebuilding, were performed to improve the model. Water molecules were added after R_{free} had decreased to below 30%. The last rounds of refinement were carried out again with Refmac5. Statistics for data collection, phasing and refinement are shown in Table 1.

Sequence and structure analysis

Sequence databases were searched with PSI-BLAST,[46] and multiple sequence alignments were generated with CLUSTALW.[47] The programs DALI[24] and CATH[27] were used to search for structurally similar and functionally related proteins, and for protein domain fold classification. These searches were done with the entire MltA structure, as well as with the two individual domains (domain A: residues 3–104, 244–337; domain B: residues 105–243).

Modelling of glycan

To obtain a model of sMltA bound with a short glycan chain, the crystal structure of sMltA was superimposed onto that of endoglucanase V in complex with two cellotriose molecules bound to subsites −4, −3, −2 and +1,+2,+3 (PDB entry 4ENG[30]). Next, the two cellotrioses were transferred to the equivalent positions in sMltA and linked together through glycosidic bonds *via* an additional glucose residue placed at subsite −1, thus creating a celloheptaose molecule. The 2-OH groups of celloheptaose were then replaced by 2-acetamido groups to generate chitoheptaose. The sMltA-chitoheptaose model was energy-minimized using CNS[45] to remove bad contacts, restraining the positions of the sugar rings at subsites −2 and +1, and restricting protein atom movement to side-chains with atoms within a 6 Å cut-off distance from the glycan heptamer. Since the sugar residue at the non-reducing end of the chitoheptaose (equivalent to the −4 sugar in the EGV–sugar complex) was completely outside the groove, not having any contact with protein atoms, it was removed from the model. Then, the 3-OH moieties of the sugar moieties occupying subsites −3, −1 and +2 were replaced with O-linked lactate groups to generate the final model of sMltA bound with $(MurNAc\text{-}GlcNAc)_3$.

Site-directed mutagenesis and expression

Site-directed mutagenesis of the MltA mutants (D261A, D297A and D308A) was performed with the QuickChange™ site-directed mutagenesis kit (Stratagene), following the manufacturer's protocol. For each mutant, two synthetic complementary mutagenic DNA oligomer primers were used (synthesized by Sigma-Genosys Ltd) to substitute Asp (codon: GAT) with Ala (codon: GCC). As sense primers, we used for D261A 5′-GCG TCA GTT GCC TCT **GCC** CGT TCC ATT ATT CCG-3′, for D297A 5′-CTG ATG GTG GCG CTG **GCC** GTC GGT GGT GCA ATC-3′ and for D308A 5′-ATC AAA GGC CAA CAC TTC **GCC** ATC TAT CAA GGG ATC GGG-3′, and as anti-sense primers we used for D261A 5′-CGG AAT AAT GGA ACG **GGC** AGA GGC AAC TGA CGC-3′, for D297A 5′-GAT TGC ACC ACC GAC **GGC** CAG CGC CAC CAT CAG-3′ and for D308A 5′-CCC GAT CCC TTG ATA GAT **GGC** GAA GTG TTG GCC TTT GAT-3′. PCR amplifications were carried out in a GeneAmp PCR System 2400, using the pMSS vector as a template for the PCR amplification.[37] Mutant plasmids were transferred to *E. coli* (122-1) competent cells. The *E. coli* (122-1) cells that grew on agar plates supplemented with kanamycin (50 μg/ml) were used for further work. Nucleotide sequencing was done to verify the correctness of the entire sequence. Expression and purification of the mutants was carried out as described for sMltA.[37]

Activity measurements

The sMltA proteins (native and mutants) were assessed for their ability to degrade both insoluble murein sacculi and isolated $(GlcNAc\text{-}MurNAc)_n$-GlcNAc-1,6-anhydro-MurNAc glycan strands, missing the peptide moieties. The activity of the sMltA proteins on insoluble murein sacculi was measured as the release of soluble radioactivity from [^{3}H]m-diaminopimelic acid-labelled murein sacculi.[48] Labelled murein sacculi (2.5 μg, 5000 cpm) were incubated in test buffer (10 mM Tris–maleate (pH 5.2), 10 mM magnesium chloride, 50 mM sodium chloride,

0.02% (w/v) sodium azide,) for 30 min at 30 °C with 5 μg of MltA variants in a total volume of 100 μl. Then 100 μl of 1% (v/v) cetyltrimethyl ammonium bromide (CTAB) was added and the samples were incubated on ice for 20 min to precipitate the high molecular mass material. After centrifugation (16,000*g*, 15 min), the released soluble products were quantified by measuring the radioactivity in a 100 μl aliquot of the supernatant by liquid scintillation counting.

The activity of sMltA on isolated poly(MurNAc-GlcNAc) strands was determined as described.[21] Briefly, [^{3}H]GlcNAc-labelled murein[5] was digested with human serum amidase and used as substrate for the sMltA proteins:[49] 5 μg of MltA was incubated for 30 min at 30 °C with [^{3}H]GlcNAc-labelled glycan strands (1 μg, 12,000 cpm) in test buffer (see above). The reaction was stopped by boiling the samples for 8 min. The products were separated by HPLC on a Nucleosil 300-5-C18 5 μm column (Bischoff, Leonberg, Germany), at a flow-rate of 0.8 ml/min, by 5 min elution with 100 mM sodium phosphate (pH 2.0), 5% (v/v) acetonitrile, followed by elution with 100% methanol. Radioactive glycans were detected with a scintillation flow-through detector (Canberra Packard). Under these conditions, the MltA digestion product GlcNAc-1,6-anhydroMurNAc elutes at 6.1 min and is separated from the longer glycan strands that elute together at 19.7 min.

Graphics

Figures 1(a) and 3 were made using MOLSCRIPT[50] and Raster3D.[51] Figure 4 was made using Povscript[52] and Povray†.

Protein Data Bank accession number

The experimental structure factors and coordinates of the refined sMltA model have been deposited in the Protein Data Bank with accession code 2AE0.

Acknowledgements

This work was supported by The Netherlands Foundation for Chemical Research (CW) with financial aid from The Netherlands Organization for Scientific Research (NWO).

References

1. Höltje, J. V. (1998). Growth of the stress-bearing and shape-maintaining murein sacculus of *Escherichia coli*. *Microbiol. Mol. Biol. Rev.* **62**, 181–203.
2. Dijkstra, B. W. & Thunnissen, A. M. W. H. (1994). "Holy" proteins II. The soluble lytic transglycosylase. *Curr. Opin. Struct. Biol.* **4**, 810–813.
3. Heidrich, C., Ursinus, A., Berger, J., Schwarz, H. & Höltje, J. V. (2002). Effects of multiple deletions of murein hydrolases on viability, septum cleavage, and sensitivity to large toxic molecules in *Escherichia coli*. *J. Bacteriol.* **184**, 6093–6099.
4. Höltje, J. V. (1995). From growth to autolysis: the murein hydrolases in *Escherichia coli*. *Arch. Microbiol.* **164**, 243–254.
5. Kraft, A. R., Templin, M. F. & Höltje, J. V. (1998). Membrane-bound lytic endotransglycosylase in *Escherichia coli*. *J. Bacteriol.* **180**, 3441–3447.
6. Romeis, T., Vollmer, W. & Holtje, J. V. (1993). Characterization of three different lytic transglycosylases in *Escherichia coli*. *FEMS Microbiol. Letters*, **111**, 141–146.
7. Blackburn, N. T. & Clarke, A. J. (2001). Identification of four families of peptidoglycan lytic transglycosylases. *J. Mol. Evol.* **52**, 78–84.
8. Dijkstra, A. J. (1997). The soluble lytic transglycosylase family of *Escherichia coli*, *in vitro* activity *versus in vivo* function. PhD thesis, University of Groningen.
9. Templin, M. F., Edwards, D. H. & Höltje, J. V. (1992). A murein hydrolase is the specific target of bulgecin in *Escherichia coli*. *J. Biol. Chem.* **267**, 20039–20043.
10. Imada, A., Kintaka, K., Nakao, M. & Shinagawa, S. (1982). Bulgecin, a bacterial metabolite which in concert with beta-lactam antibiotics causes bulge formation. *J. Antibiot.* **35**, 1400–1403.
11. Nakao, M., Yukishige, K., Kondo, M. & Imada, A. (1986). Novel morphological changes in gram-negative bacteria caused by combination of bulgecin and cefmenoxime. *Antimicrob. Agents Chem.* **30**, 414–417.
12. Thunnissen, A. M. W. H., Dijkstra, A. J., Kalk, K. H., Rozeboom, H. J., Engel, H., Keck, W. & Dijkstra, B. W. (1994). Doughnut-shaped structure of a bacterial muramidase revealed by X-ray crystallography. *Nature*, **367**, 750–753.
13. van Asselt, E. J., Thunnissen, A. M. W. H. & Dijkstra, B. W. (1999). High resolution crystal structures of the *Escherichia coli* lytic transglycosylase Slt70 and its complex with a peptidoglycan fragment. *J. Mol. Biol.* **291**, 877–898.
14. van Asselt, E. J., Dijkstra, A. J., Kalk, K. H., Takacs, B., Keck, W. & Dijkstra, B. W. (1999). Crystal structure of *Escherichia coli* lytic transglycosylase Slt35 reveals a lysozyme-like catalytic domain with an EF-hand. *Structure*, **7**, 1167–1180.
15. Thunnissen, A. M. W. H., Isaacs, N. W. & Dijkstra, B. W. (1995). The catalytic domain of a bacterial lytic transglycosylase defines a novel class of lysozymes. *Proteins: Struct. Funct. Genet.* **22**, 245–258.
16. Davies, G. & Henrissat, B. (1995). Structures and mechanisms of glycosyl hydrolases. *Structure*, **3**, 853–859.
17. Evrard, C., Fastrez, J. & Declercq, J. P. (1998). Crystal structure of the lysozyme from bacteriophage lambda and its relationship with V and C-type lysozymes. *J. Mol. Biol.* **276**, 151–164.
18. Leung, A. K. W., Duewel, H. S., Honek, J. F. & Berghuis, A. M. (2001). Crystal structure of the lytic transglycosylase from bacteriophage lambda in complex with hexa-*N*-acetylchitohexaose. *Biochemistry*, **40**, 5665–5673.
19. Thunnissen, A. M. W. H., Rozeboom, H. J., Kalk, K. H. & Dijkstra, B. W. (1995). Structure of the 70-kDa soluble lytic transglycosylase complexed with bulgecin A. Implications for the enzymatic mechanism. *Biochemistry*, **34**, 12729–12737.
20. van Asselt, E. J., Kalk, K. H. & Dijkstra, B. W. (2000). Crystallographic studies of the interactions of *Escherichia coli* lytic transglycosylase Slt35 with peptidoglycan. *Biochemistry*, **39**, 1924–1934.
21. Ursinus, A. & Höltje, J. V. (1994). Purification and properties of a membrane-bound lytic transglycosylase from *Escherichia coli*. *J. Bacteriol.* **176**, 338–343.
22. LoConte, L., Ailey, B., Hubbard, T. J., Brenner, S. E.,

† http://www.povray.org/

Murzin, A. G. & Chothia, C. (2000). SCOP: a structural classification of proteins database. *Nucl. Acids Res.* **28**, 257–259.
23. Castillo, R. M., Mizuguchi, K., Dhanaraj, V., Albert, A., Blundell, T. L. & Murzin, A. G. (1999). A six-stranded double-psi beta barrel is shared by several protein superfamilies. *Structure*, **7**, 227–236.
24. Holm, L. & Sander, C. (1995). Dali: a network tool for protein structure comparison. *Trends Biochem. Sci.* **20**, 478–480.
25. Stoldt, M., Wohnert, J., Ohlenschlager, O., Gorlach, M. & Brown, L. R. (1999). The NMR structure of the 5S rRNA E-domain-protein L25 complex shows preformed and induced recognition. *EMBO J.* **18**, 6508–6521.
26. Fedorov, R., Meshcheryakov, V., Gongadze, G., Fomenkova, N., Nevskaya, N., Selmer, M. *et al*. (2001). Structure of ribosomal protein TL5 complexed with RNA provides new insights into the CTC family of stress proteins. *Acta Crystallog. sect. D*, **57**, 968–976.
27. Orengo, C. A., Michie, A. D., Jones, S., Jones, D. T., Swindells, M. B. & Thornton, J. M. (1997). CATH, a hierarchic classification of protein domain structures. *Structure*, **5**, 1093–1108.
28. Schou, C., Rasmussen, G., Kaltoft, M. B., Henrissat, B. & Schulein, M. (1993). Stereochemistry, specificity and kinetics of the hydrolysis of reduced cellodextrins by nine cellulases. *Eur. J. Biochem.* **217**, 947–953.
29. Davies, G. J., Dodson, G. G., Hubbard, R. E., Tolley, S. P., Dauter, Z., Wilson, K. S. *et al*. (1993). Structure and function of endoglucanase V. *Nature*, **365**, 362–364.
30. Davies, G. J., Tolley, S. P., Henrissat, B., Hjort, C. & Schulein, M. (1995). Structures of oligosaccharide-bound forms of the endoglucanase V from *Humicola insolens* at 1.9 Å resolution. *Biochemistry*, **34**, 16210–16220.
31. Park, Y. J., Kim, H. S. & Jeffrey, G. A. (1971). The crystal structure of 1,6-anhydro-β-D-glucopyranose. *Acta Crystallog. sect. B*, **27**, 220–227.
32. Vocadlo, D. J., Davies, G. J., Laine, R. & Withers, S. G. (2001). Catalysis by hen egg-white lysozyme proceeds *via* a covalent intermediate. *Nature*, **412**, 835–838.
33. Terwisscha van Scheltinga, A. C., Armand, S., Kalk, K. H., Isogai, A., Henrissat, B. & Dijkstra, B. W. (1995). Stereochemistry of chitin hydrolysis by a plant chitinase/lysozyme and X-ray structure of a complex with allosamidin: evidence for substrate assisted catalysis. *Biochemistry*, **34**, 15619–15623.
34. Tews, I., Terwisscha van Scheltinga, A. C., Perrakis, A., Wilson, K. S. & Dijkstra, B. W. (1997). Substrate assisted catalysis unifies two families of chitinolytic enzymes. *J. Am. Chem. Soc.* **119**, 7954–7959.
35. Ludvigsen, S. & Poulsen, F. M. (1992). Three-dimensional structure in solution of barwin, a protein from barley seed. *Biochemistry*, **31**, 8783–8789.
36. Cosgrove, D. J. (2000). Loosening of plant cell walls by expansins. *Nature*, **407**, 321–326.
37. van Straaten, K. E., Dijkstra, B. W. & Thunnissen, A. M. W. H. (2004). Purification, crystallization and preliminary X-ray analysis of the lytic transglycosylase MltA from *Escherichia coli*. *Acta Crystallog. sect. D*, **60**, 758–760.
38. Doublié, S. (1997). Preparation of selenomethionyl proteins for phase determination. *Methods Enzymol.* **276**, 523–530.
39. Gerchman, S. E., Graziano, V. & Ramakrishnan, V. (1994). Expression of chicken linker histones in *E. coli*: sources of problems and methods for overcoming some of the difficulties. *Protein Expr. Purif.* **5**, 242–251.
40. Otwinowski, Z. & Minor, W. (1997). Processing of X-ray diffraction data collection in oscillation mode. *Methods Enzymol.* **276**, 307–326.
41. Weeks, C. M. & Miller, R. (1999). The design and implementations of SnB V2.0. *J. Appl. Crystallog.* **32**, 120–124.
42. Terwilliger, T. (2004). SOLVE and RESOLVE: automated structure solution, density modification and model building. *J. Synchrotron Radiat.* **11**, 49–52.
43. McRee, D. E. (1999). XtalView/Xfit-a versatile program for manipulating atomic coordinates and electron density. *J. Struct. Biol.* **125**, 156–165.
44. Murshudov, G. N., Vagin, A. A. & Dodson, E. J. (1997). Refinement of macromolecular structures by the maximum-likelihood method. *Acta Crystallog. sect. D*, **53**, 240–255.
45. Brünger, A. T., Adams, P. D., Clore, G. M., DeLano, W. L., Gros, P., Grosse-Kunstleve, R. W. *et al*. (1998). Crystallography & NMR system: a new software suite for macromolecular structure determination. *Acta Crystallog. sect. D*, **54**, 905–921.
46. Altschul, S. F., Madden, T. L., Schaffer, A. A., Zhang, J., Zhang, Z., Miller, W. & Lipman, D. J. (1997). Gapped BLAST and PSI-BLAST: a new generation of protein database search programs. *Nucl. Acids Res.* **25**, 3389–3402.
47. Thompson, J. D., Higgins, D. G. & Gibson, T. J. (1994). ClustalW: improving the sensitivity of progressive multiple sequence alignment through sequence weighting, position-specific gap penalties and weight matrix choice. *Nucl. Acids Res.* **22**, 4673–4680.
48. Kusser, W. & Schwarz, U. (1980). *Escherichia coli* murein transglycosylase. Purification by affinity chromatography and interaction with polynucleotides. *Eur. J. Biochem.* **103**, 277–281.
49. Harz, H., Burgdorf, K. & Höltje, J. V. (1990). Isolation and separation of the glycan strands from murein of *Escherichia coli* by reversed-phase high-performance liquid chromatography. *Anal. Biochem.* **190**, 120–128.
50. Kraulis, P. (1991). MOLSCRIPT: a program to produce both detailed and schematic plots of protein structures. *J. Appl. Crystallog.* **24**, 946–950.
51. Merritt, E. A. & Murphy, M. E. (1994). Raster3D Version 2.0. A program for photorealistic molecular graphics. *Acta Crystallog. sect. D*, **50**, 869–873.
52. Fenn, T. D., Ringe, D. & Petsko, G. A. (2003). POVScript+: a program for model and data visualization using persistence of vision ray-tracing. *J. Appl. Crystallog.* **36**, 944–947.
53. Gouet, P., Courcelle, E., Stuart, D. I. & Metoz, F. (1999). ESPript: analysis of multiple sequence alignments in PostScript. *Bioinformatics*, **15**, 305–308.

Edited by M. Guss

(Received 28 May 2005; received in revised form 21 July 2005; accepted 26 July 2005)
Available online 11 August 2005